Radio Channel Modeling for UAV Communication Over Cellular Networks

Rafhael Amorim, Huan Nguyen, Preben Mogensen, István Z. Kovács, Jeroen Wigard, and Troels B. Sørensen

***Abstract*—The main goal of this letter is to obtain models for path loss exponents and shadowing for the radio channel between airborne unmanned aerial vehicles (UAVs) and cellular networks. In this pursuit, field measurements were conducted in live LTE networks at the 800 MHz frequency band, using a commercial UAV. Our results show that path loss exponent decreases as the UAV moves up, approximating freespace propagation for horizontal ranges up to tens of kilometers at UAV heights around 100 m. Our findings support the need of height-dependent parameters for describing the propagation channel for UAVs at different heights.**

***Index Terms*—UAV, drone, path loss, propagation, channel modelling, drone communication, field measurement, air-to-ground, radio channel measurements.**

I. Introduction

UNMANNED aerial vehicles (UAVs), also known as drones, have been used for military applications for more than 20 years. More recently, technological developments regarding batteries, electronics and lightweight materials have made UAVs more accessible to the public, creating a boom in the market of small and medium scale UAVs. However, due to concerns with public safety most of their applications are still limited by countries regulations to visual-line-of-sight (VLOS) ranges and maximum heights between 100 and 150 m [1].

Emerging UAV applications present potential to reduce risk and cost for many commercial activities [2], but they would require larger operational ranges. The research community is putting efforts into creating solutions for a safe integration of drones in the airspace for beyond-VLOS flight ranges. An essential element in this is the development of a reliable communication link between the pilot/controller and the UAV.

The cellular networks are natural candidates to provide not only this link, known as CNPC (control and non-payload communication) [1], [3], [4] or C2 (communication and control link) [5], but also to serve data traffic for applications such as live streaming or sensor readings. Mobile operators already have ground infrastructures implemented and a ubiquitous coverage that can be adapted to serve such air-to-infrastructure links [6]. To study the feasibility of cellular-based communication for drones, a good understanding of the propagation channel between UAVs and ground stations is required. It is reasonable to assume the channel will present different behaviors for an aerial user when compared to a regular ground user. UAVs flying above rooftops, vegetation and terrain elevations, are more likely to observe radio path clearance to the base stations in the surrounding areas and therefore more likely to experience line-of-sight (LOS) propagations [6] for larger distances resulting in higher level of interference from a larger number of surrounding BSs [7].

Some efforts to characterize the aerial channel were presented by Matolak and Sun [8], [9], where measurements were performed using single dedicated links at 900 MHz and 5 GHz bands, with large drones flying at heights between 500 m and 2 km, but the effect of height dependency is not directly assessed, neither heights below 150m, which are expected to be heavily used by commercial drones in the near future.

Some previous studies have suggested it is important to obtain a model that accounts for the dependency observed in the propagation channel to UE heights [3], [4]. Goddemeier *et al.* [10] present a modification to the two-ray model which introduces variation in the path loss exponent according to the UE height, based on GSM and UMTS measurements collected by a stationary balloon located at 1900 m of the serving base station. Measurements in LTE using a flying UAV were reported in [7] and results suggest there is a clearance of the radio path, obtained with higher UE heights, reduces the shadowing variation while it increases the received signal power from the interfering cells and the number of visible neighboring cells, but no propagation model is presented.

The present work differs from the previous studies, as it directly assesses the effects of the LTE UAV-UE heights in the path loss exponent and shadowing variation, and proposes a height dependent modeling for both. A wider range of distances and diverse surrounding base stations are assessed using a flying LTE UAV-UE, connected to two real LTE networks at 800 MHz in Denmark.

This letter is organized as follows. The setup used in the trials and the data processing methodology are introduced in Section II. Section III present the measurements results, while the modeling of the height-dependent radio propagation channel is presented in Section IV. This letter follows with the conclusion in Section V.

II. Measurement Setup and Data Processing

A measurement campaign was performed in October 2016, using the setup reported in Table I. The scanner was mounted

Manuscript received April 13, 2017; accepted May 19, 2017. Date of publication May 31, 2017; date of current version August 21, 2017. The associate editor coordinating the review of this paper and approving it for publication was D. Tarchi. *(Corresponding author: Rafhael Amorim.)*

R. Amorim, H. Nguyen, and T. B. Sørensen are with the Department of Electronic Systems, Aalborg University, 9220 Aalborg, Denmark (e-mail: rma@es.aau.dk; hcn@es.aau.dk; tbs@es.aau.dk).

P. Mogensen is with the Department of Electronic Systems, Aalborg University, 9220 Aalborg, Denmark, and also with Nokia Bell Labs, 9220 Aalborg, Denmark (e-mail: pm@es.aau.dk).

I. Z. Kovács and J. Wigard are with Nokia Bell Labs, 9220 Aalborg, Denmark (e-mail: istvan.kovacs@nokia-bell-labs.com; jeroen.wigard@nokia-bell-labs.com).

Digital Object Identifier 10.1109/LWC.2017.2710045

TABLE I
MEASUREMENTS SETUP INFORMATION

Setup Information	Value
Location	Fyn, Southern Denmark
Meas. Device	R&S® TSMA[1]
Technology	LTE
Band (MHz)	800
UAV Flight Speed	15 km/h
Avg. Sampling Rate	4 - 9 Hz
UAV-UE Antenna	Dipole
UAV Heights (m)	15, 30, 60, 120
Drive Test Height (m)	1.5

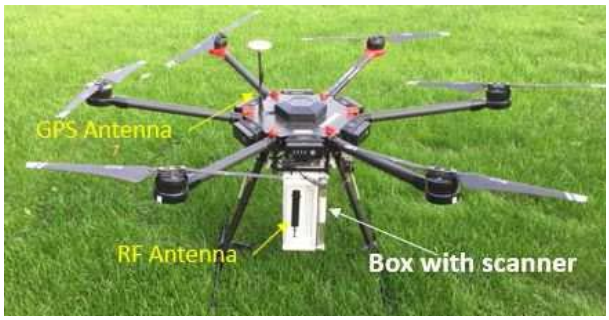

Fig. 1. UAV-Scanner Mounting used for the measurements.

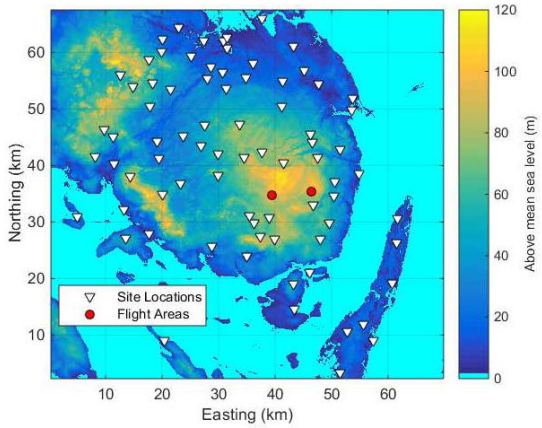

Fig. 2. Site Locations and Terrain Profile for the measurement campaign in Fyn, Denmark.

underneath a commercial UAV connected to a dipole antenna, whose gain is small and assumed negligible for the purpose of this analysis, vertically placed as depicted in Fig. 1. The scanner is capable of reporting radio measurements from up to 32 cells per recorded sample. The reports include the UAV GPS locations and reference signal received power (RSRP) and physical cell ID (PCI) from each detected cell. The measurements were repeated for two different Danish operators with independent networks and their results were combined to produce the outcome presented in Section III. The terrain profile and the location of sites in a radius of 35 km around the flight zone are showed in Fig. 2. The UAV was set to fly over two circular paths of 500m diameter, set 7 km apart from each other (see Fig. 2). The UAV heights, measured from the take-off spot, according to the maximum limits allowed by local regulations. On ground, a reference drive-test (DT) was also performed on the nearby roads around the flying paths. During the drive test, the antenna is mounted on top of a car at 1.5 m height. With distances around 2 km from the closest BS, the propagation path is most of the time blocked by surrounding trees, buildings and hills, and therefore non line-of-sight is dominant condition in the drive test.

Each RSRP sample recorded by the scanner, R_i, recorded from a site at a distance d_i in meters, was translated into a path loss sample PL_i, according to the following equation

$$PL_i = P_{T_x} + G_a(\theta, \phi) - R_i \quad [dB], \tag{1}$$

where P_{T_x} represents the average transmitted power per reference symbol in the network, and G_a is the antenna gain for the azimuthal θ and elevation ϕ angles measured between the base station and the UAV. The antenna gain is calculated through the horizontal interpolation algorithm (HPI) applied over the horizontal and vertical antenna diagrams, obtained from manufacturers. Example of antennas used in the networks include: Kathrein 80010699, Kathrein 80010647V01, among others. The calculation of elevation considers BS's and UAV's heights altogether with terrain topography. At the highest flight level, 120m, the UAV is flying above cellular base stations, which are usually downtilted for optimized ground coverage. However, distances ranges in this letter are limited to 1-22km and elevation angles were in the range of 0.25 to 2.9 degrees. When the geometrical elevation angle is added to antennas tilt, the maximum angle to the main beam of base station antennas is around 10 degrees, with more than 95% of samples below 7.5 degrees. In order to avoid the roll off region of the antenna patterns and miscompensation of the antenna gains in Eq. (1), samples lying outside the -6dB vertical and horizontal lobes of the BS antenna pattern were filtered out from the analysis.

The effect of fast fading components in the measurements are mitigated by obtaining the local mean of samples for PL_i using windows of length equal to 40λ [11], where λ represents the radio wavelength at 800 MHz. The pair of averaged path loss samples and distances, (PL'_j, d'_j) were then used to obtain a regression, in the least square sense, to fit a log-distance alpha-beta (AB) model, widely used in [12]:

$$PL_{est}(d) = \alpha 10 \log_{10}(d) + \beta + X_\sigma \quad [\text{dB}]. \tag{2}$$

In Eq. (2), PL_{est} represents the estimated path loss for a receiver located at a 3-D distance d (in meters) from the transmitter; α represents the path loss exponent and β is the intercept point with the line $d = 1$ m. Finally, X_σ is a random variable that accounts for shadowing variation modeled with normal distribution and standard deviation σ, assumed equal to the standard deviation of the regression residuals [12].

At very large distance, some path loss samples might be cropped, as the received power is not high enough to overcome the noise plus interference level so that the broadcast channel can be successfully decoded. The sensitivity level (PL_{sens}), i.e., path loss value when cropping occurs, is height-dependent as the interference increases with the flight height (it will become more evident in Section III). This cropping negatively affects the path loss analysis: it causes the path loss slope to be skewed downward, thus underestimating path loss exponent. Therefore, a threshold distance ($d_{max}(hu)$) is

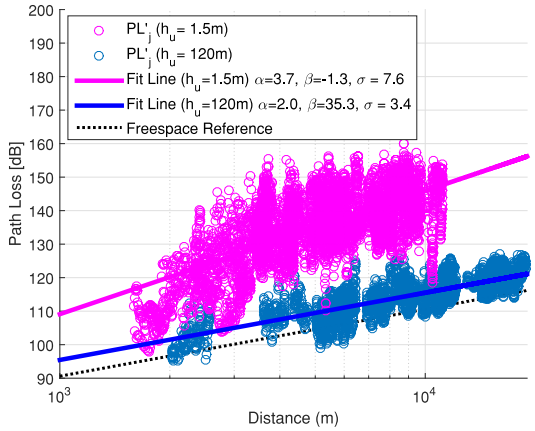

Fig. 3. Path loss vs Distance - Measurement Results and regression model for UAV heights h_u = 1.5 and 120 m.

applied, where we removed samples greater than this distance to avoid the bias due to saturated samples. The choice of the threshold distance is important, as if it is set too high, the slope will experience the effect of cropping; if too low, a significant number of points will be removed from the analysis, and this might compromise the statistical significance of the regression values.

In this letter the threshold distance is selected as follows: First P_{sens} was defined as 99%-percentile of all measured PL'_j for a given height. The 99%-ile was chosen in order not to make the assumed sensitivity value too low due to outliers. Then, $d_{max}(h_u)$ was iteratively increased until the following stopping criteria is reached:

$$PL_{est}(d_{max}) \leq PL_{sens} - \sigma, \tag{3}$$

where $PL_{est}(d_{max})$ represents the estimated value for the path loss at d_{max}, using the regression presented in eq (2), using all points that satisfy $d'_j \leq d_{max}(h_u)$.. Assuming a Gaussian shadowing distribution, $\approx 15\%$ of the samples at $d_{max}(h_u)$ are expected to be above $PL_{est}(d_{max}(h_u)) + \sigma$ (in the cropping region). The expected down-bias in the path loss slope using this criteria is within 0.1, and therefore, negligible for the later remarks presented in this letter.

III. Measurement Results

The results obtained through the methodology described in Section IV are presented in Fig. 3, where it is possible to see that there is a clear reduction in path loss exponents as h_u increases, from 3.7 at ground level to 2.0 at 120 m. It results in significant differences in the path loss attenuation, specially for larger distances: for 3D distances close to 10 km the signal attenuation is 20 dB higher on ground level compared to the measurements at 120m.

The summary of the results for the other flight tests can be appreciated in Table II that supports the expectations of better radio clearance at higher heights, with the path loss exponent approaching free space propagation at higher flight levels [7]. In practical terms, such observation implies an expected increase in the interference level observed by UAVs, as well as a higher number of neighbor base stations being affected by UAV's transmissions. This claim is also supported by the average number of detected cells per sample that increased from 5.1 (DT) to 16.9 (120m). This height dependent behavior in the distance range and number of significant interference sources complies with previous results reported in [7]. It is also worth mentioning that the measurements suggest the signal power threshold increased at higher heights in all measured routes. This is exemplified by the value of PL_{sens} in Table II. This behavior might be attributed to the higher interference levels, and it indicates the number of significant interfering sites could be even higher, as some might not be identified due to falling short of the required signal-to-interference plus noise ratio (SINR) level.

TABLE II
Measurements Summary

h_u	Reg. Model Parameters			Avg. # Cells	PL_{sens} (dB)	d_{max} (km)
	α	β (dB)	$\sigma(dB)$			
1.5	3.7	-1.3	7.7	5.1	155.4	11.1
15	2.9	7.4	6.2	6.1	135.6	13.6
30	2.5	20.4	5.2	7.6	130.7	16.5
60	2.1	32.8	4.4	11.6	126.2	17.4
120	2.0	35.3	3.4	16.9	125.9	22.2

Another finding that goes in line with the radio path clearance with height regards the observed values for the shadowing variation. For DT measurements it is approximately 7.7, which is aligned with reference values in [13] for ground level measurements. As the UAV moves up this value decreases up to 3.4 dB, indicating a significant reduction in the shadowing variation. Part of the remaining variation might be attributed to the non-omni directional pattern of the receiver antenna and self-shadowing components.

IV. Path Loss Modelling and Discussion

The results in Section III made clear the propagation environment is significantly different for airborne UAVs and ground level users. Based on such observations, and in the work in [3], [4], [7], and [10], it is proposed here an extension of the model in Eq. (2) using height-dependent parameters. Path loss exponents should decay with increases in UAV heights. In this letter, a logarithmic regression was used to obtain a group of height-dependent parameters to be used in eq. (2). The logarithmic function was chosen assuming height-related radio path clearance, i.e., the path loss exponents reduction, is more prominent to small increments in elevation at low heights, where there are more concentration of buildings, vegetations and other obstacles. The height-dependent models are found in equations (4)–(6).

$$\alpha(h_u) = \max\left(p_{\alpha_1} + p_{\alpha_2}\log_{10}(h_u),\ 2\right), \tag{4}$$

$$\beta(h_u) = p_{\beta_1} + p_{\beta_2}\log_{10}(\min(h_u,\ h_{FSPL})) \quad [dB] \tag{5}$$

$$\sigma(h_u) = p_{\sigma_1} + p_{\sigma_2}\log_{10}(\min(h_u,\ h_{FSPL})) \quad [dB], \tag{6}$$

where h_{FSPL} is the height where free space propagation is assumed ($\alpha = 2.0$). The values of p_1 and p_2 obtained based on the reported measurements are exposed in Table III. Such parameters modelling serves as a reference for rural scenarios, and are valid for ranges limited to 1.5 m $\leq h_u \leq$ 120 m and

TABLE III
HEIGHT-DEPENDENT MODEL PARAMETERS

Parameter	p_1	p_2
α	3.9	-0.9
β	-8.5	20.5
σ	8.2	-2.1

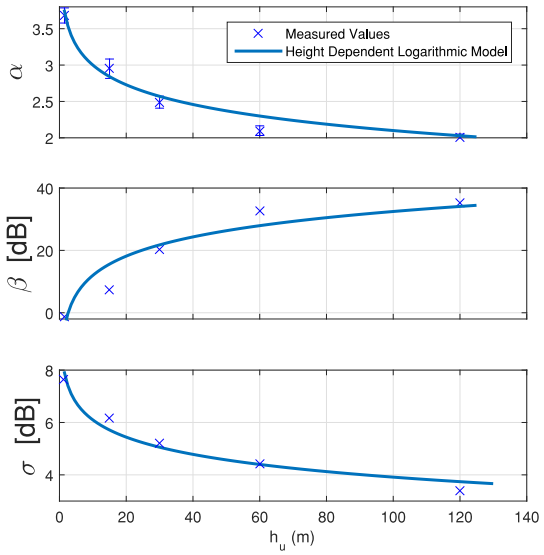

Fig. 4. Height dependent models for the regression parameters of eq. (2).

distance ranges similar to those in Table II, in a lightly hilly rural environment, with base stations height between 20 and 50 meters.

Using the slope and intercept estimation given by the height dependent model, and applying it to all measurements collected, the average offset between the measured samples and the estimated ones is equal to -0.3 dB, and the standard deviation for all heights was kept under the same values presented in Table II. It means the proposed height-dependent model is capable of providing a good model for the measured data, at expense of just two optimization variables per parameter.

A visual example of the height dependent model using the parameters in Table III, is shown in Fig. 4. The 95% confidence interval for the value of α estimated on the measured data is also shown, assuming X_σ to be Gaussian distributed (in which case the estimate is Student t-distributed [14]). These values suggest the difference among the exponents at higher levels ($h_u = 60$ or 120 m) compared to those at lower levels ($h_u = 1.5$ or 15) is statistically significant.

V. CONCLUSION

This letter analyzed a set of live network measurements conducted with a radio network LTE scanner attached to an airborne UAV. Flights were conducted at heights compliant with current regulations, up to 120m. The results for the path loss exponents and the shadowing standard deviations imply better radio clearance as the UAV moves up. This finding is corroborated by the increase in the average number of detected cells at higher levels. A practical consequence of these observations is an expected SINR degradation at higher elevations, to be evaluated in future works.

In order to investigate the interference problem and evaluate mechanisms to deal with it, system level simulations are required. The main contribution of this letter is presented in Section IV. It proposes that path loss and shadowing parameters for airbone UAVs connected to cellular networks must follow height-dependent models, as a more efficient way of performing spatial prediction, as the radio path becomes more unobstructed with increases in height.

ACKNOWLEDGMENT

The authors would like to thank the team from DroneFyn Denmark which assisted in this research by conducting the UAV Flights. The authors would also like to acknowledge the important contribution made by Rohde & Schwarz, which provided the TSMA scanner used in the measurements.

REFERENCES

[1] "Roadmap for the integration of civil remotely-piloted aircraft systems into the European aviation system," EUROCONTROL, Brussels, Belgium, Tech. Rep., 2013. [Online]. Available: https://publicintelligence.net/eu-rpa-roadmap/
[2] "The future of drones according to the AT&T foundry," AT&T Foundry, Palo Alto, CA, USA, Ericsson, Stockholm, Sweden, and Rocket Space, San Francisco, CA, USA, Tech. Rep., Oct. 2016. [Online]. Available: https://www.qualcomm.com/invention/technologies/lte/advanced-pro/cellular-drone-communication
[3] "Consideration on the channel model for LTE-based aerial vehicles," ZTE Microelectron., Tongji Univ., Shanghai, China, Tech. Rep. R1-1705163, Apr. 2017.
[4] "Evaluation scenarios and channel models for drones," Alcatel-Lucent Shanghai Bell Labs, Shanghai, China, Nokia, Espoo, Finland, Tech. Rep. R1-1704430, Apr. 2017.
[5] "Integration of civil unmanned aircraft systems (UAS) in the national airspace system (NAS) roadmap," U.S. Dept. Transp., FAA, Washington, DC, USA, Tech. Rep. 2012-AJG-502, 2013.
[6] K. Welch, "Evolving cellular technologies for safer drone operation," Qualcomm 5G White Paper Present., San Diego, CA, USA, Tech. Rep., Oct. 2016.
[7] B. V. D. Bergh, A. Chiumento, and S. Pollin, "LTE in the sky: Trading off propagation benefits with interference costs for aerial nodes," *IEEE Commun. Mag.*, vol. 54, no. 5, pp. 44–50, May 2016.
[8] D. W. Matolak and R. Sun, "Air-ground channel characterization for unmanned aircraft systems: The hilly suburban environment," in *Proc. IEEE 80th Veh. Technol. Conf. (VTC Fall)*, Vancouver, BC, Canada, Sep. 2014, pp. 1–5.
[9] D. W. Matolak and R. Sun, "Air-ground channel characterization for unmanned aircraft systems: The near-urban environment," in *Proc. IEEE Mil. Commun. Conf. (MILCOM)*, Tampa, FL, USA, Oct. 2015, pp. 1656–1660.
[10] N. Goddemeier, K. Daniel, and C. Wietfeld, "Role-based connectivity management with realistic air-to-ground channels for cooperative UAVs," *IEEE J. Sel. Areas Commun.*, vol. 30, no. 5, pp. 951–963, Jun. 2012.
[11] W. C. Y. Lee, "Estimate of local average power of a mobile radio signal," *IEEE Trans. Veh. Technol.*, vol. VT-34, no. 1, pp. 22–27, Feb. 1985.
[12] T. Rappaport, *Wireless Communications: Principles and Practice* (Prentice Hall Communications Engineering and Emerging Technologies Series). Upper Saddle River, NJ, USA: Prentice-Hall, 2002.
[13] V. Erceg *et al.*, "An empirically based path loss model for wireless channels in suburban environments," *IEEE J. Sel. Areas Commun.*, vol. 17, no. 7, pp. 1205–1211, Jul. 1999.
[14] D. G. Altman, D. Machin, T. N. Bryant, and M. J. Gardner, *Statistics With Confidence: Confidence Intervals and Statistical Guidelines*. London, U.K.: BMJ Books, Feb. 2000.